

Three-loop nonsinglet matching coefficients for heavy quark currents

Manuel Egner^{1,*}, Matteo Fael^{1,†}, Fabian Lange^{1,2,‡}, Kay Schönwald^{1,§} and Matthias Steinhauser^{1,||}

¹*Institut für Theoretische Teilchenphysik, Karlsruhe Institute of Technology (KIT),
76128 Karlsruhe, Germany*

²*Institut für Astroteilchenphysik, Karlsruhe Institute of Technology (KIT),
76344 Eggenstein-Leopoldshafen, Germany*



(Received 29 March 2022; accepted 19 May 2022; published 8 June 2022)

We compute the matching coefficients between QCD and nonrelativistic QCD for external vector, axial-vector, scalar, and pseudoscalar currents up to three-loop order. We concentrate on the nonsinglet contributions and present precise numerical results with an accuracy of about ten digits. For the vector current the results from Marquard *et al.* [Phys. Rev. D **89**, 034027 (2014)] are confirmed, increasing the accuracy by several orders of magnitude.

DOI: 10.1103/PhysRevD.105.114007

I. INTRODUCTION

The construction of effective field theories with quantum chromodynamics (QCD) as a starting point is a very successful approach in order to describe a number of different phenomena, which involve different energy scales following a large hierarchy. A popular example in this context is nonrelativistic QCD (NRQCD), which describes systems with two heavy quarks moving with small relative velocity. Prominent applications are the threshold production of top-quark pairs in electron-positron annihilation and properties of charmonium and bottomonium bound states. For comprehensive reviews we refer to Refs. [1–4].

For the construction of the effective theories one considers Green functions in the full and effective theories and requires that they are equal up to corrections in the small expansion parameter, which in the case of NRQCD are power-suppressed terms in the inverse heavy quark mass m . Such calculations, usually referred to as matching calculations, fix the couplings of the operators in the effective theory. These couplings are typically denoted as matching coefficients.

In this paper we consider QCD and NRQCD as full and effective theories and compute the matching coefficients of external vector, axial-vector, scalar, and pseudoscalar currents

up to three-loop order in perturbation theory. For this purpose it is necessary to compute vertex corrections involving one of the currents and a quark-anti-quark pair. We concentrate on the nonsinglet contributions where the external currents directly couple to the external quarks. Sample Feynman diagrams up to three loops are shown in Fig. 1.

From the phenomenological point of view the vector current is certainly most important. It enters as building block to the threshold production of top-quark pairs [5] and the decay width of the $\Upsilon(1S)$ meson [6,7]. Its Abelian contribution is an important ingredient to the hyperfine splitting of positronium [8]. As possible applications of the scalar and pseudoscalar matching coefficient one could imagine the decay of CP -even or CP -odd Higgs bosons with mass M into two quarks with mass $m \approx M/2$.

Starting point for the matching calculation are the vector, axial-vector, scalar, and pseudoscalar currents in QCD, which we define as

$$\begin{aligned} j_v^\mu &= \bar{\psi}\gamma^\mu\psi, & j_a^\mu &= \bar{\psi}\gamma^\mu\gamma_5\psi, \\ j_s &= \bar{\psi}\psi, & j_p &= \bar{\psi}i\gamma_5\psi. \end{aligned} \quad (1)$$

Note that the anomalous dimensions of the vector and axial-vector current are zero, whereas j_s and j_p involve nontrivial renormalization constants.

Expanding the spinors in Eq. (1) for $|\vec{p}| \ll m$, where \vec{p} is the momentum of the antiquark in the final state, one finds the currents in the effective theory,

$$\begin{aligned} \tilde{j}_v^k &= \phi^\dagger \sigma^k \chi, & \tilde{j}_a^k &= \frac{1}{2m} \phi^\dagger [\sigma^k, \vec{p} \cdot \vec{\sigma}] \chi, \\ \tilde{j}_s &= -\frac{1}{m} \phi^\dagger \vec{p} \cdot \vec{\sigma} \chi, & \tilde{j}_p &= -i\phi^\dagger \chi, \end{aligned} \quad (2)$$

where ϕ and χ are two-component Pauli spinors.

*manuel.egner@kit.edu
†matteo.fael@kit.edu
‡fabian.lange@kit.edu
§kay.schoenwald@kit.edu
||matthias.steinhauser@kit.edu

Published by the American Physical Society under the terms of the Creative Commons Attribution 4.0 International license. Further distribution of this work must maintain attribution to the author(s) and the published article's title, journal citation, and DOI. Funded by SCOAP³.

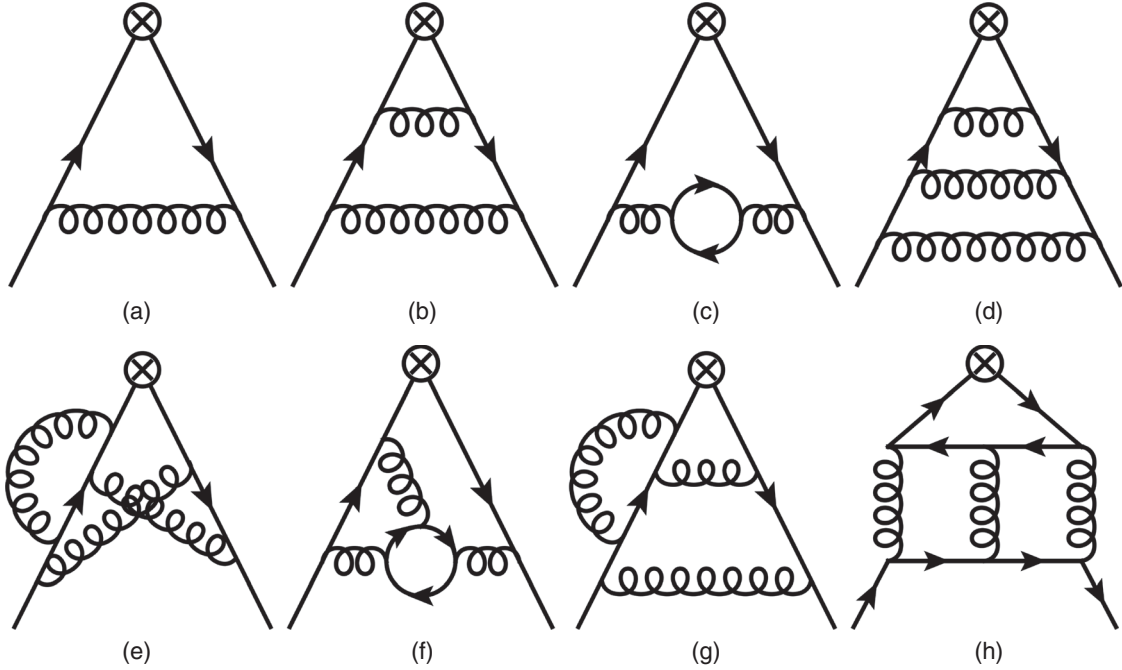


FIG. 1. Sample Feynman diagrams at one-, two-, and three-loop order for the current-quark-anti-quark vertex corrections. Solid and curly lines denote quarks and gluons, respectively. The cross represents the coupling to the external current. In this work we only consider nonsinglet contributions (a)–(g) and neglect the singlet contributions (h).

The currents in Eqs. (1) and (2) are used to form renormalized vertex functions with two external on shell quarks, which we denote by $\Gamma_x(q_1, q_2)$ and $\tilde{\Gamma}_x$ with $x \in \{v, a, s, p\}$, respectively. q_1 and q_2 correspond to the momenta of the quark and antiquark with $q_1^2 = q_2^2 = m^2$, where m is the quark mass. We apply an asymptotic expansion around $s = 4m^2$ [9,10], where s is the momentum squared of the external current, which leads to

$$Z_2 Z_x \Gamma_x(q_1, q_2) = c_x \tilde{Z}_2 \tilde{Z}_x^{-1} \tilde{\Gamma}_x + \dots \quad (3)$$

The ellipses denote terms suppressed by at least two inverse powers of the heavy quark mass. It is understood that $\Gamma_x(q_1, q_2)$ is expressed in terms of the heavy quark mass in the on shell scheme and the strong coupling in the $\overline{\text{MS}}$ scheme. Z_2 and \tilde{Z}_2 are the on shell wave function renormalization constants. Z_2 is needed up to three loops [11,12], whereas $\tilde{Z}_2 = 1$ since the quantum corrections in NRQCD only involve scaleless integrals that are set to zero in dimensional regularization. Also for $\tilde{\Gamma}_x$ only tree-level contributions are needed since the soft, potential, and ultrasoft contributions are present on both sides of Eq. (3) and cancel such that only the hard contribution of $\Gamma_x(q_1, q_2)$ has to be computed. Z_x is the renormalization constant of the current in full QCD, which is given by $Z_v = Z_a = 1$ and $Z_s = Z_p = Z_m$. Here Z_m is the on shell quark mass renormalization constant defined via $m = Z_m m^0$, where m_0 is the bare heavy quark mass. \tilde{Z}_x is the renormalization constant of the current in NRQCD, which is determined from the infrared divergences of c_x . \tilde{Z}_x deviates from

1 starting at order α_s^2 . The computation of the matching coefficient c_x is the main purpose of this work.

Two-loop corrections to c_v have been computed for the first time in Refs. [13,14] and in Ref. [15] two-loop corrections to all four currents have been considered, including the singlet contributions. Three-loop corrections to c_v have been computed in Refs. [16–18]. In these works the reduction to master integrals has been performed analytically. However, most of the master integrals have only been computed numerically with the help of FIESTA [19]. As a consequence the coefficients of some color structures are only known with an uncertainty of a few percent. This is sufficient for most phenomenological applications. It is nevertheless desirable to have an independent cross check with improved accuracy. This is provided in this work.

In the next section we provide details on our calculation and describe our method to extract the matching coefficient from results for the form factors. In Sec. III we present our results for the matching coefficients and the anomalous dimension of the currents in the effective theory. Section IV contains a brief summary.

II. TECHNICAL DETAILS

For the computation of the hard part of the vertex diagrams we apply the method developed in Ref. [20]. We profit from the findings of Refs. [21,22] where results for massive form factors with external vector, axial-vector, scalar, and pseudoscalar currents have been computed. They can be decomposed into six form factors given by

$$\begin{aligned}
\Gamma_\mu^v(q_1, q_2) &= F_1^v(s)\gamma_\mu - \frac{i}{2m} F_2^v(s)\sigma_{\mu\nu}q^\nu, \\
\Gamma_\mu^a(q_1, q_2) &= F_1^a(s)\gamma_\mu\gamma_5 - \frac{1}{2m} F_2^a(s)q_\mu\gamma_5, \\
\Gamma^s(q_1, q_2) &= mF^s(s), \\
\Gamma^p(q_1, q_2) &= imF^p(s)\gamma_5,
\end{aligned} \tag{4}$$

where $\sigma^{\mu\nu} = i[\gamma^\mu, \gamma^\nu]/2$ and s is the invariant mass of the external current. The quantity $\Gamma_x(q_1, q_2)$ in Eq. (3) is obtained from the hard part of the form factors evaluated at $s = 4m^2$ through

$$\begin{aligned}
\Gamma_v &= (F_1^v + F_2^v)|_{\text{hard}, s=4m^2}, \\
\Gamma_a &= F_1^a|_{\text{hard}, s=4m^2}, \\
\Gamma_s &= F^s|_{\text{hard}, s=4m^2}, \\
\Gamma_p &= F^p|_{\text{hard}, s=4m^2},
\end{aligned} \tag{5}$$

which is discussed in more detail in the remainder of this section.

The basic idea of Ref. [20] is to construct expansions of the master integrals for various values of s/m^2 with the help of the corresponding differential equations. The unconstrained coefficients of the expansions are fixed by matching two neighboring expressions at an intermediate point. The starting point in Refs. [21,22] is $s = 0$ where all master integrals can be computed analytically. In order to arrive at the threshold $s = 4m^2$ we perform expansions for $s/m^2 = 1, 2, 5/2, 3, 7/2$, and 4.

The expansion around $s/m^2 = 4$ uses the variable

$$x = \sqrt{4 - \frac{s}{m^2}}. \tag{6}$$

It contains both even and odd powers of x accompanied by $\ln(x)$ terms, since it comprises the contributions from all regions present close to threshold. In particular, each loop momentum can have one of the following scalings [9]¹:

- (i) hard (h): $k_0 \sim m, k_i \sim m$,
- (ii) potential (p): $k_0 \sim x^2 \cdot m, k_i \sim x \cdot m$,
- (iii) soft (s): $k_0 \sim x \cdot m, k_i \sim x \cdot m$,
- (iv) ultrasoft (u): $k_0 \sim x^2 \cdot m, k_i \sim x^2 \cdot m$.

For the matching coefficients we only need the region where all loop momenta are hard. Here only even powers of x and no $\ln(x)$ terms are present.

Using the scalings from above, we see that in each region the integral is given as $x^{-n\epsilon}$ multiplied by a Taylor expansion in x , with an integer n , which can be derived from the scaling of the loop momenta in the respective region. Here $\epsilon = (4-d)/2$ where d is the space-time dimension. We can insert this ansatz into the system of differential equations for the master integrals and obtain a

¹Note that in Ref. [9] the variable $y = 1 - s/(4m^2) = x^2/4$ has been used.

system of linear equations for the expansion coefficients. For each region the system is reduced to a small set of undetermined boundary constants with the help of a version of KIRA [23,24] with FIREFLY [25,26] optimized for solving systems without variables. After summing the contributions from all regions we obtain again the results for the master integrals in full kinematics. We can therefore numerically match the yet undetermined boundary constants with the numerical results computed in Ref. [21]. Substituting the numerical solutions into the ansatz for the $x^{-0\epsilon}$ scaling provides the master integrals in the hard expansion.

Let us in the following discuss the calculation in more detail. At two-loop order we find the following scalings for the different regions:

- (i) $x^{-0\epsilon}$: (h-h),
- (ii) $x^{-2\epsilon}$: (h-p), (h-s),
- (iii) $x^{-4\epsilon}$: (h-u), (p-p), (s-s), (p-s),
- (iv) $x^{-6\epsilon}$: (p-u), (s-u),
- (v) $x^{-8\epsilon}$: (u-u),

where the list on the right of the colon specifies the scaling of the two loop momenta. Some of the combinations might vanish due to the presence of scaleless integrals. However, in our approach we do not have to pay attention to this. Since only the spacial parts get continued into $(d-1)$ dimensions, potential and soft regions of the loop momenta lead to the same ϵ -dimensional scalings. The pure ultrasoft region $\sim x^{-8\epsilon}$ does not contribute, which we checked by an explicit calculation. For the two-loop calculation we therefore have to consider four independent expansions. Note that the individual regions contributing to one of the $x^{-n\epsilon}$ scalings might develop higher poles in the dimensional regulator ϵ than the sum. These higher poles lead to Sudakov-like double logarithms that are not present in the threshold expansion considered here. We therefore do not have to extend the ansatz to higher poles in ϵ compared to the full calculation in Ref. [21].

At three loop order we have the scalings

- (i) $x^{-0\epsilon}$: (h-h-h),
- (ii) $x^{-2\epsilon}$: (h-h-p), (h-h-s),
- (iii) $x^{-4\epsilon}$: (h-h-u), (h-p-p), (h-s-s), (h-p-s),
- (iv) $x^{-6\epsilon}$: (h-p-u), (h-s-u), (p-p-p), (p-p-s), (p-s-s), (s-s-s),
- (v) $x^{-8\epsilon}$: (h-u-u), (u-p-p), (u-p-s), (u-s-s),
- (vi) $x^{-10\epsilon}$: (u-u-p), (u-u-s),
- (vii) $x^{-12\epsilon}$: (u-u-u),

which means that we have to construct six independent expansions since the pure-ultrasoft contribution vanishes. After the reduction to boundary constants we are left with (568, 125, 248, 402, 236, 51) undetermined coefficients for the scalings $x^{-0\epsilon}, \dots, x^{-10\epsilon}$. They can be reduced by utilizing information about the master integrals from the full calculation. On the one hand, we know some integrals analytically, especially those which do not depend on s . They can be fixed from the expansion around $s = 0$. Furthermore, some of the ϵ poles also do not have a s dependence and thus also they are available from the calculation performed for $s = 0$. On the

other hand, we know the leading power in x for each integral from the full result. This knowledge implies relations between the boundary constants from different regions which leads to a reduction of the number of independent boundary constants from 1630 to 578. They are determined as follows: After obtaining the symbolic expansions for each region we equate the sum of all regions with the numerical evaluation of the full result at $s = 3.75m^2$ from Ref. [21] and solve the resulting linear system for the 578 boundary constants. In particular all 568 coefficients from the pure-hard regions of all 422 master integrals are obtained by this procedure, whereas the regions which scale as x^{-ne} with $n > 0$ cannot be disentangled. This is sufficient for the application in the present paper.

Let us mention that in case one wants to construct results for each individual region further information is needed. It can be obtained by determining for each region of every master integral the leading power in x . Here the program ASYM [27,28] can be used. In this way one obtains relations for each individual region instead of only for the sum of all of them.

Next we insert the hard regions of the master integrals into the amplitudes for the form factors. It contains terms scaling with inverse powers of $(s - 4m^2)$ from the reduction of the master integrals with full kinematics. It is a nontrivial check that the limit $s \rightarrow 4m^2$ exists. In fact we have checked that all

inverse powers of $(s - 4m^2)$ have coefficients below 3×10^{-11} , which is the precision of our calculation. Inserting the form factors into Eq. (5) we finally obtain the vertex functions Γ_x entering the matching equation (3). As a further check we keep the QCD gauge parameter ξ and observe that it vanishes after renormalization.

III. THREE-LOOP MATCHING COEFFICIENTS

Once all ingredients for the left-hand side of Eq. (3) are available we can solve it for c_x order by order in α_s . At one-loop order all quantities with a tilde on the right-hand side are equal to 1. At order α_s^2 infrared divergences are left on the left-hand side, which are absorbed into \tilde{Z}_x . Finally, at order α_s^3 one has to take care of the interference term of \tilde{Z}_x^{-1} and the one-loop result of c_x , which is needed up to order ϵ . The remaining infrared divergences are again absorbed into \tilde{Z}_x . We parametrize the perturbative results in this section by the strong coupling in the effective theory with n_l active quark flavors, which we denote by $\alpha_s^{(n_l)}$.

Let us in a first step provide the results for the renormalization constants that are obtained by subtracting the remaining infrared divergences in a minimal way. For the vector current we have

$$\begin{aligned} \tilde{Z}_v = 1 &+ \left(\frac{\alpha_s^{(n_l)}(\mu)}{\pi}\right)^2 \frac{C_F \pi^2}{\epsilon} \left(\frac{1}{12} C_F + \frac{1}{8} C_A\right) + \left(\frac{\alpha_s^{(n_l)}(\mu)}{\pi}\right)^3 C_F \pi^2 \left\{ C_F^2 \left[\frac{5}{144\epsilon^2} + \left(\frac{43}{144} - \frac{1}{2} l_2 + \frac{5}{48} L_\mu\right) \frac{1}{\epsilon} \right] \right. \\ &+ C_F C_A \left[\frac{1}{864\epsilon^2} + \left(\frac{113}{324} + \frac{1}{4} l_2 + \frac{5}{32} L_\mu\right) \frac{1}{\epsilon} \right] + C_A^2 \left[-\frac{1}{16\epsilon^2} + \left(\frac{2}{27} + \frac{1}{4} l_2 + \frac{1}{24} L_\mu\right) \frac{1}{\epsilon} \right] \\ &\left. + T n_l \left[C_F \left(\frac{1}{54\epsilon^2} - \frac{25}{324\epsilon}\right) + C_A \left(\frac{1}{36\epsilon^2} - \frac{37}{432\epsilon}\right) \right] + C_F T n_h \frac{1}{60\epsilon} \right\} + \mathcal{O}(\alpha_s^4), \end{aligned} \quad (7)$$

which agrees with the explicit calculations in the effective theory from Refs. [14,16,29,30]. In Eq. (7) $C_F = (N_c^2 - 1)/(2N_c)$ and $C_A = 2N_c$ are the quadratic Casimir operators of the $SU(N_c)$ gauge group in the fundamental and adjoint representation, respectively, n_l is the number of massless quark flavors, and $T = 1/2$. Furthermore we have $L_\mu = \ln(\mu^2/m^2)$ and $l_2 = \ln(2)$.

For the remaining three currents our results read

$$\begin{aligned} \tilde{Z}_a = 1 &+ \left(\frac{\alpha_s^{(n_l)}(\mu)}{\pi}\right)^2 \frac{C_F \pi^2}{\epsilon} \left(\frac{1}{24} C_A + \frac{5}{48} C_F\right) + \left(\frac{\alpha_s^{(n_l)}(\mu)}{\pi}\right)^3 C_F \pi^2 \left\{ C_F^2 \left(\frac{215}{864} - \frac{l_2}{3}\right) \frac{1}{\epsilon} \right. \\ &+ C_F C_A \left[-\frac{25}{576\epsilon^2} + \left(\frac{1}{18} l_2 + \frac{35}{576} L_\mu + \frac{1433}{5184}\right) \frac{1}{\epsilon} \right] + C_A^2 \left[-\frac{1}{48\epsilon^2} + \left(\frac{5}{36} l_2 + \frac{1}{72} L_\mu + \frac{17}{324}\right) \frac{1}{\epsilon} \right] \\ &\left. + T n_l \left[C_F \left(\frac{5}{216\epsilon^2} - \frac{83}{1296\epsilon}\right) + C_A \left(\frac{1}{108\epsilon^2} - \frac{53}{1296\epsilon}\right) \right] \right\}, \\ \tilde{Z}_s = 1 &+ \left(\frac{\alpha_s^{(n_l)}(\mu)}{\pi}\right)^2 \frac{C_F \pi^2}{\epsilon} \left(\frac{1}{24} C_A + \frac{1}{6} C_F\right) + \left(\frac{\alpha_s^{(n_l)}(\mu)}{\pi}\right)^3 C_F \pi^2 \left\{ C_F^2 \left(\frac{65}{216} - \frac{1}{3} l_2\right) \frac{1}{\epsilon} \right. \\ &+ C_F C_A \left[-\frac{7}{96\epsilon^2} + \left(\frac{461}{1296} + \frac{1}{18} l_2 + \frac{25}{288} L_\mu\right) \frac{1}{\epsilon} \right] + C_A^2 \left[-\frac{1}{48\epsilon^2} + \left(\frac{17}{324} + \frac{5}{36} l_2 + \frac{1}{72} L_\mu\right) \frac{1}{\epsilon} \right] \\ &\left. + T n_l \left[C_F \left(\frac{1}{27\epsilon^2} - \frac{29}{324\epsilon}\right) + C_A \left(\frac{1}{108\epsilon^2} - \frac{53}{1296\epsilon}\right) \right] \right\}, \end{aligned}$$

$$\begin{aligned} \tilde{Z}_p = & 1 + \left(\frac{\alpha_s^{(n_l)}(\mu)}{\pi}\right)^2 \frac{C_F \pi^2}{\epsilon} \left(\frac{1}{8} C_A + \frac{1}{4} C_F\right) + \left(\frac{\alpha_s^{(n_l)}(\mu)}{\pi}\right)^3 C_F \pi^2 \left\{ C_F^2 \left[\frac{5}{144 \epsilon^2} + \left(\frac{31}{144} - \frac{1}{2} l_2 + \frac{5}{48} L_\mu\right) \frac{1}{\epsilon} \right] \right. \\ & + C_F C_A \left[-\frac{5}{96 \epsilon^2} + \left(\frac{199}{432} + \frac{1}{4} l_2 + \frac{29}{96} L_\mu\right) \frac{1}{\epsilon} \right] + C_A^2 \left[-\frac{1}{16 \epsilon^2} + \left(\frac{2}{27} + \frac{1}{4} l_2 + \frac{1}{24} L_\mu\right) \frac{1}{\epsilon} \right] \\ & \left. + T n_l \left[C_F \left(\frac{1}{18 \epsilon^2} - \frac{11}{108 \epsilon}\right) + C_A \left(\frac{1}{36 \epsilon^2} - \frac{37}{432 \epsilon}\right) \right] + C_F T n_h \frac{1}{60 \epsilon} \right\}. \end{aligned} \quad (8)$$

Note that our method only provides numerical results for the pole parts. However, the precision is sufficiently high such that the analytic results can be reconstructed using the partial sum of least squares (PSLQ) algorithm [31].

The renormalization constants are related to the anomalous dimensions via

$$\gamma_x = \frac{d \ln(\tilde{Z}_x)}{d \ln(\mu)}, \quad (9)$$

which leads to

$$\gamma_x = -4 \left(\frac{\alpha_s^{(n_l)}}{\pi}\right)^2 \tilde{Z}_x^{(2,-1)} - 6 \left(\frac{\alpha_s^{(n_l)}}{\pi}\right)^3 \tilde{Z}_x^{(3,-1)} + \mathcal{O}(\alpha_s^4), \quad (10)$$

where $\tilde{Z}_x^{(a,b)}$ denotes the contribution to \tilde{Z} at order $\alpha_s^a \epsilon^b$.

For the perturbative expansion of c_x we set the renormalization scale of the strong coupling constant to $\mu^2 = m^2$ and write

$$\begin{aligned} c_x = & 1 + \frac{\alpha_s^{(n_l)}(m)}{\pi} c_x^{(1)} + \left(\frac{\alpha_s^{(n_l)}(m)}{\pi}\right)^2 c_x^{(2)} \\ & + \left(\frac{\alpha_s^{(n_l)}(m)}{\pi}\right)^3 c_x^{(3)} + \mathcal{O}(\alpha_s^4). \end{aligned} \quad (11)$$

The three-loop coefficient is further decomposed according to the color structures as

$$\begin{aligned} c_x^{(3)} = & C_F [C_F^2 c_{FFF}^x + C_F C_A c_{FFA}^x + C_A^2 c_{FAA}^x \\ & + T n_l (C_F c_{FFL}^x + C_A c_{FAL}^x + T n_h c_{FHL}^x + T n_l c_{FLL}^x) \\ & + T n_h (C_F c_{FFH}^x + C_A c_{FAH}^x + T n_h c_{FHH}^x)] \\ & + \text{singlet terms}. \end{aligned} \quad (12)$$

In the following we present result for c_x where for completeness also the one- and two-loop results are shown. For the vector current our results read:

$$\begin{aligned} c_v^{(1)} = & -2 C_F, \\ c_v^{(2)} = & \left(-\frac{151}{72} + \frac{89}{144} \pi^2 - \frac{5}{6} \pi^2 l_2 - \frac{13}{4} \zeta(3)\right) C_A C_F \\ & + \left(\frac{23}{8} - \frac{79}{36} \pi^2 + \pi^2 l_2 - \frac{1}{2} \zeta(3)\right) C_F^2 \\ & + \left(\frac{22}{9} - \frac{2}{9} \pi^2\right) C_F T n_h + \frac{11}{18} C_F T n_l \\ & - \frac{1}{2} \pi^2 \left(\frac{1}{2} C_A + \frac{1}{3} C_F\right) C_F L_\mu, \\ c_{FFF}^v = & 36.49486246 + \left(-\frac{9}{16} + \frac{3}{2} l_2\right) \pi^2 L_\mu - \frac{5}{32} \pi^2 L_\mu^2, \\ c_{FFA}^v = & -188.0778417 + \left(-\frac{59}{108} - \frac{3}{4} l_2\right) \pi^2 L_\mu - \frac{47}{576} \pi^2 L_\mu^2, \\ c_{FAA}^v = & -97.73497327 + \left(-\frac{2}{9} - \frac{3}{4} l_2\right) \pi^2 L_\mu + \frac{1}{6} \pi^2 L_\mu^2, \\ c_{FFL}^v = & 46.69169291 + \frac{25}{108} \pi^2 L_\mu - \frac{1}{18} \pi^2 L_\mu^2, \\ c_{FAL}^v = & 39.62371855 + \frac{37}{144} \pi^2 L_\mu - \frac{1}{12} \pi^2 L_\mu^2, \\ c_{FHL}^v = & -\frac{557}{162} + \frac{26}{81} \pi^2, \\ c_{FLL}^v = & -\frac{163}{162} - \frac{4}{27} \pi^2, \\ c_{FFH}^v = & -0.8435622912 - \frac{1}{20} \pi^2 L_\mu, \\ c_{FAH}^v = & -0.1024741615, \\ c_{FHH}^v = & -\frac{427}{162} + \frac{158}{2835} \pi^2 + \frac{16}{9} \zeta(3). \end{aligned} \quad (13)$$

The coefficient of the logarithmic contributions and the coefficients c_{FHL}^v and c_{FLL}^v have been reconstructed using our numerical expressions. They agree with the results presented in Ref. [17]. Our numerical precision is not sufficient to obtain the analytic expressions for c_{FFH}^v , which we take from Ref. [17]. For all coefficients presented in numerical form we have a precision of at least ten digits, which is a significant improvement. For example, for the nonfermionic coefficients the results in Ref. [17] read $c_{FFF}^v = 36.55(0.53)$, $c_{FFA}^v = -188.10(0.83)$, and $c_{FAA}^v = -97.81(0.38)$.

For the remaining three currents we have

$$\begin{aligned}
c_a^{(1)} &= -C_F, \\
c_a^{(2)} &= \left(-\frac{9}{8}\zeta(3) + \frac{35}{144}\pi^2 - \frac{101}{72} - \frac{7}{12}\pi^2 l_2\right) C_A C_F \\
&\quad + \left(-\frac{27}{16}\zeta(3) - \frac{9}{8}\pi^2 + \frac{23}{24} + \frac{19}{24}\pi^2 l_2\right) C_F^2 \\
&\quad + \left(\frac{20}{9} - \frac{2}{9}\pi^2\right) C_F T n_h + \frac{7}{18} C_F T n_l \\
&\quad + \pi^2 \left(-\frac{1}{12} C_A - \frac{5}{24} C_F\right) C_F L_\mu, \\
c_{FFF}^a &= -4.764274486 + \left(-\frac{155}{288} + l_2\right) \pi^2 L_\mu, \\
c_{FFA}^a &= -83.88648515 + \left(-\frac{1289}{1728} - \frac{1}{6} l_2\right) \pi^2 L_\mu \\
&\quad + \frac{115}{1152} \pi^2 L_\mu^2, \\
c_{FAA}^a &= -63.00619439 + \left(-\frac{17}{108} - \frac{5}{12} l_2\right) \pi^2 L_\mu \\
&\quad + \frac{1}{18} \pi^2 L_\mu^2, \\
c_{FFL}^a &= 28.13543651 + \frac{83}{432} \pi^2 L_\mu - \frac{5}{72} \pi^2 L_\mu^2, \\
c_{FAL}^a &= 23.17119085 + \frac{53}{432} \pi^2 L_\mu - \frac{1}{36} \pi^2 L_\mu^2, \\
c_{FHL}^a &= -\frac{415}{162} + \frac{20}{81} \pi^2, \\
c_{FLL}^a &= -\frac{65}{162} - \frac{2}{27} \pi^2, \\
c_{FFH}^a &= 0.8971357511, \\
c_{FAH}^a &= -0.2169123942, \\
c_{FHH}^a &= -0.01136428050,
\end{aligned} \tag{14}$$

$$\begin{aligned}
c_s^{(1)} &= -\frac{1}{2} C_F, \\
c_s^{(2)} &= \left(-\frac{5}{4}\zeta(3) + \frac{1}{48}\pi^2 + \frac{49}{144} - \frac{1}{2}\pi^2 l_2\right) C_A C_F \\
&\quad + \left(-\frac{11}{4}\zeta(3) - \frac{37}{48}\pi^2 + \frac{5}{16} + \frac{1}{2}\pi^2 l_2\right) C_F^2 \\
&\quad + \left(\frac{121}{36} - \frac{1}{3}\pi^2\right) C_F T n_h - \frac{5}{36} C_F T n_l \\
&\quad + \pi^2 \left(-\frac{1}{12} C_A - \frac{1}{3} C_F\right) C_F L_\mu, \\
c_{FFF}^s &= -11.17444530 + \left(-\frac{53}{72} + l_2\right) \pi^2 L_\mu,
\end{aligned}$$

$$\begin{aligned}
c_{FFA}^s &= -83.13918787 + \left(-\frac{443}{432} - \frac{1}{6} l_2\right) \pi^2 L_\mu + \frac{101}{576} \pi^2 L_\mu^2, \\
c_{FAA}^s &= -67.24288900 + \left(-\frac{17}{108} - \frac{5}{12} l_2\right) \pi^2 L_\mu \\
&\quad + \frac{1}{18} \pi^2 L_\mu^2, \\
c_{FFL}^s &= 30.10118322 + \frac{29}{108} \pi^2 L_\mu - \frac{1}{9} \pi^2 L_\mu^2, \\
c_{FAL}^s &= 21.41321398 + \frac{53}{432} \pi^2 L_\mu - \frac{1}{36} \pi^2 L_\mu^2, \\
c_{FHL}^s &= -\frac{157}{81} + \frac{5}{27} \pi^2, \\
c_{FLL}^s &= \frac{73}{324} - \frac{1}{27} \pi^2, \\
c_{FFH}^s &= 1.879249909, \\
c_{FAH}^s &= -0.3740808359, \\
c_{FHH}^s &= 0.007237324266,
\end{aligned} \tag{15}$$

$$\begin{aligned}
c_p^{(1)} &= -\frac{3}{2} C_F, \\
c_p^{(2)} &= \left(-3\zeta(3) + \frac{17}{48}\pi^2 - \frac{17}{48} - \pi^2 l_2\right) C_A C_F \\
&\quad + \left(-\frac{9}{2}\zeta(3) - \frac{79}{48}\pi^2 + \frac{29}{16} + \pi^2 l_2\right) C_F^2 \\
&\quad + \left(\frac{43}{12} - \frac{1}{3}\pi^2\right) C_F T n_h + \frac{1}{12} C_F T n_l \\
&\quad + \pi^2 \left(-\frac{1}{4} C_A - \frac{1}{2} C_F\right) C_F L_\mu, \\
c_{FFF}^p &= -16.65729478 + \left(\frac{5}{48} + \frac{3}{2} l_2\right) \pi^2 L_\mu - \frac{5}{32} \pi^2 L_\mu^2, \\
c_{FFA}^p &= -181.0487647 + \left(-\frac{145}{144} - \frac{3}{4} l_2\right) \pi^2 + \frac{1}{192} \pi^2 L_\mu^2, \\
c_{FAA}^p &= -104.3591595 + \left(-\frac{2}{9} - \frac{3}{4} l_2\right) \pi^2 L_\mu + \frac{1}{6} \pi^2 L_\mu^2, \\
c_{FFL}^p &= 51.93841187 + \frac{11}{36} \pi^2 L_\mu - \frac{1}{6} \pi^2 L_\mu^2, \\
c_{FAL}^p &= 39.92104383 + \frac{37}{144} \pi^2 L_\mu - \frac{1}{12} \pi^2 L_\mu^2, \\
c_{FHL}^p &= -\frac{76}{27} + \frac{7}{27} \pi^2, \\
c_{FLL}^p &= -\frac{41}{108} - \frac{1}{9} \pi^2, \\
c_{FFH}^p &= 3.081762039 - \frac{1}{20} \pi^2 L_\mu, \\
c_{FAH}^p &= -0.8953812450, \\
c_{FHH}^p &= 0.06984121227.
\end{aligned} \tag{16}$$

For the axial-vector, scalar, and pseudoscalar current the terms proportional to n_l and n_l^2 can be found in Ref. [32]. There, the nonlogarithmic terms of the coefficients c_{FFL}^x and c_{FAL}^x only have a precision of two significant digits, whereas we have a precision of at least ten digits. Our analytic results for c_{FHL}^x and c_{FLL}^x agree with [32].

After specifying the number of colors to three we have for $\mu^2 = m^2$ and $n_h = 1$

$$\begin{aligned}
c_v &\approx 1 - \frac{\alpha_s^{(n_l)}}{\pi} \cdot 2.66667 + \left(\frac{\alpha_s^{(n_l)}}{\pi}\right)^2 [-44.5510 + 0.407407n_l] \\
&\quad + \left(\frac{\alpha_s^{(n_l)}}{\pi}\right)^3 [-2090.33 + 120.661n_l - 0.822779n_l^2] \\
&\quad + \text{singlet terms,} \\
c_a &\approx 1 - \frac{\alpha_s^{(n_l)}}{\pi} \cdot 1.33333 + \left(\frac{\alpha_s^{(n_l)}}{\pi}\right)^2 [-29.3816 + 0.259259n_l] \\
&\quad + \left(\frac{\alpha_s^{(n_l)}}{\pi}\right)^3 [-1214.40 + 71.3101n_l - 0.377439n_l^2] \\
&\quad + \text{singlet terms,} \\
c_s &\approx 1 - \frac{\alpha_s^{(n_l)}}{\pi} \cdot 0.666667 \\
&\quad + \left(\frac{\alpha_s^{(n_l)}}{\pi}\right)^2 [-30.2266 - 0.0925926n_l] \\
&\quad + \left(\frac{\alpha_s^{(n_l)}}{\pi}\right)^3 [-1275.89 + 69.5462n_l - 0.0467441n_l^2] \\
&\quad + \text{singlet terms,} \\
c_p &\approx 1 - \frac{\alpha_s^{(n_l)}}{\pi} \cdot 2 + \left(\frac{\alpha_s^{(n_l)}}{\pi}\right)^2 [-52.1381 + 0.0555556n_l] \\
&\quad + \left(\frac{\alpha_s^{(n_l)}}{\pi}\right)^3 [-2256.42 + 125.924n_l - 0.492084n_l^2] \\
&\quad + \text{singlet terms.} \tag{17}
\end{aligned}$$

For all four currents the quantum corrections are quite sizable. For applications in the top quark sector, i.e., for $n_l = 5$, the two- and three-loop corrections have the same order of magnitude as the one-loop term. For $n_l = 3$ and $n_l = 4$ the higher order corrections are even larger. Since the matching coefficients on their own are no physical quantities this is no principle problem. However, it shows the importance of the three-loop corrections to c_x , in particular for c_v , which has important applications in the bottom [6,7] and top sector [5]. For example, if one evaluates the decay rate for $\Upsilon(1S) \rightarrow \ell^+\ell^-$ at the scale $\mu = 3.5$ GeV the contribution of the three-loop corrections to c_v is larger than the leading order term. However, after adding the remaining third-order contributions one arrives at a net correction of about 3% [6,7].

IV. CONCLUSIONS

In this work we have computed the three-loop corrections to the QCD-NRQCD matching coefficients for external vector, axial-vector, scalar, and pseudoscalar currents. We consider the corresponding quark form factors and compute the pure-hard part of each master integral using the method of Ref. [20] supplemented with the information from expansions by regions [9]. We obtain precise numerical results for the three-loop coefficients. For the vector current we provide the first independent cross check for c_v , which has a significant numerical impact to the next-to-next-to-next-to-leading order predictions for top-quark-pair production in electron-positron annihilation close to threshold and the leptonic decay width of the $\Upsilon(1S)$ meson. Our new result is several orders of magnitude more precise. The three-loop results for c_a , c_s , and c_p are new.

ACKNOWLEDGMENTS

This research was supported by the Deutsche Forschungsgemeinschaft (DFG, German Research Foundation) under Grant No. 396021762—TRR 257 “Particle Physics Phenomenology after the Higgs Discovery.” The Feynman diagrams were drawn with the help of AXODRAW [33] and JaxoDraw [34].

-
- [1] G. T. Bodwin, E. Braaten, and G. P. Lepage, *Phys. Rev. D* **51**, 1125 (1995); **55**, 5853(E) (1997).
 - [2] N. Brambilla, A. Pineda, J. Soto, and A. Vairo, *Rev. Mod. Phys.* **77**, 1423 (2005).
 - [3] A. Pineda, *Prog. Part. Nucl. Phys.* **67**, 735 (2012).
 - [4] M. Beneke, Y. Kiyo, and K. Schuller, arXiv:1312.4791.
 - [5] M. Beneke, Y. Kiyo, P. Marquard, A. Penin, J. Piclum, and M. Steinhauser, *Phys. Rev. Lett.* **115**, 192001 (2015).
 - [6] M. Beneke, Y. Kiyo, P. Marquard, A. Penin, J. Piclum, D. Seidel, and M. Steinhauser, *Phys. Rev. Lett.* **112**, 151801 (2014).
 - [7] M. Egner, M. Fael, J. Piclum, K. Schönwald, and M. Steinhauser, *Phys. Rev. D* **104**, 054033 (2021).
 - [8] M. Baker, P. Marquard, A. A. Penin, J. Piclum, and M. Steinhauser, *Phys. Rev. Lett.* **112**, 120407 (2014).
 - [9] M. Beneke and V. A. Smirnov, *Nucl. Phys.* **B522**, 321 (1998).

- [10] V. A. Smirnov, *Springer Tracts Mod. Phys.* **177**, 1 (2002).
- [11] K. Melnikov and T. van Ritbergen, *Nucl. Phys.* **B591**, 515 (2000).
- [12] P. Marquard, L. Mihaila, J. H. Piclum, and M. Steinhauser, *Nucl. Phys.* **B773**, 1 (2007).
- [13] A. Czarnecki and K. Melnikov, *Phys. Rev. Lett.* **80**, 2531 (1998).
- [14] M. Beneke, A. Signer, and V. A. Smirnov, *Phys. Rev. Lett.* **80**, 2535 (1998).
- [15] B. A. Kniehl, A. Onishchenko, J. H. Piclum, and M. Steinhauser, *Phys. Lett. B* **638**, 209 (2006).
- [16] P. Marquard, J. H. Piclum, D. Seidel, and M. Steinhauser, *Nucl. Phys.* **B758**, 144 (2006).
- [17] P. Marquard, J. H. Piclum, D. Seidel, and M. Steinhauser, *Phys. Rev. D* **89**, 034027 (2014).
- [18] P. Marquard, J. H. Piclum, D. Seidel, and M. Steinhauser, *Phys. Lett. B* **678**, 269 (2009).
- [19] A. V. Smirnov, *Comput. Phys. Commun.* **204**, 189 (2016).
- [20] M. Fael, F. Lange, K. Schönwald, and M. Steinhauser, *J. High Energy Phys.* **09** (2021) 152.
- [21] M. Fael, F. Lange, K. Schönwald, and M. Steinhauser, *Phys. Rev. Lett.* **128**, 172003 (2022).
- [22] M. Fael, F. Lange, K. Schönwald, and M. Steinhauser, Three-loop massive form factors: non-singlet case (to be published).
- [23] P. Maierhöfer, J. Usovitsch, and P. Uwer, *Comput. Phys. Commun.* **230**, 99 (2018).
- [24] J. Klappert, F. Lange, P. Maierhöfer, and J. Usovitsch, *Comput. Phys. Commun.* **266**, 108024 (2021).
- [25] J. Klappert and F. Lange, *Comput. Phys. Commun.* **247**, 106951 (2020).
- [26] J. Klappert, S. Y. Klein, and F. Lange, *Comput. Phys. Commun.* **264**, 107968 (2021).
- [27] A. Pak and A. Smirnov, *Eur. Phys. J. C* **71**, 1626 (2011).
- [28] B. Jantzen, A. V. Smirnov, and V. A. Smirnov, *Eur. Phys. J. C* **72**, 2139 (2012).
- [29] B. A. Kniehl, A. A. Penin, V. A. Smirnov, and M. Steinhauser, *Phys. Rev. Lett.* **90**, 212001 (2003); **91**, 139903(E) (2003).
- [30] M. Beneke, Y. Kiyo, and A. A. Penin, *Phys. Lett. B* **653**, 53 (2007).
- [31] H. R. P. Ferguson, D. H. Bailey, and S. Arno, *Math. Comput.* **68**, 351 (1999).
- [32] J. H. Piclum, Heavy quark threshold dynamics in higher order, Dissertation, Hamburg University 2007.
- [33] J. A. M. Vermaseren, *Comput. Phys. Commun.* **83**, 45 (1994).
- [34] D. Binosi and L. Theußl, *Comput. Phys. Commun.* **161**, 76 (2004).